GEOPHYSICAL RESEARCH LETTERS, VOL. 38, L08501, doi:10.1029/2011GL046680, 2011

Nonlinear interaction between ocean tides and the Larsen C Ice Shelf system

Matt A. King,[1] Keith Makinson,[2] and G. Hilmar Gudmundsson[2]

Received 5 January 2011; revised 2 March 2011; accepted 16 March 2011; published 21 April 2011.

[1] We report on three GPS records of flow of the Larsen C Ice Shelf, spanning 2 months to 2 years. Variations in speed are evident at periods from a few hours to ~182 days, including semi-diurnal, diurnal and ~14.76 days. At fortnightly periods the ice shelf varies by ±10% from its long-term speed but at diurnal timescales it is up to ±100%. A nonlinear relationship between ocean tides and velocity is required to explain the observed variations in flow. As an initial examination we model flow as a non-linear function of basal shear stress including tidal perturbations in the ice shelf grounding zone and show that the major features of the observations are reproduced, notably the long-period signal largely absent from the vertical tidal signal. Alternative explanations are discussed. These observations demonstrate that the ice shelf system is highly sensitive to relatively modest changes in forcing at its boundaries. **Citation:** King, M. A., K. Makinson, and G. H. Gudmundsson (2011), Nonlinear interaction between ocean tides and the Larsen C Ice Shelf system, *Geophys. Res. Lett.*, *38*, L08501, doi:10.1029/2011GL046680.

1. Introduction

[2] The Larsen C Ice Shelf (LCIS) has come under increased scrutiny since the demise of the more northerly Larsen A and B ice shelves and suggestion that it may also, and in the near future, be subject to instability [*Scambos et al.*, 2004]. This is of particular importance as glaciers feeding into former parts of Larsen Ice Shelf have shown substantial and prolonged speedup and thinning [e.g., *Rignot et al.*, 2004] thereby increasing sea level and freshening the ocean. Consequently, significant effort is going into assessing its stability and modeling its dynamics [e.g., *Glasser et al.*, 2009]. Understanding the connection between the grounded and floating ice and then robustly modeling its evolution is particularly critical.

[3] Here we report on new Global Positioning System (GPS) data collected on LCIS from which we derived coordinate time series. These provide new insights into the coupling of the grounded and floating ice in its grounding zone and allow us to estimate basal boundary conditions near the LCIS grounding zone.

2. Data Analysis

[4] We collected GPS data at the sites shown in Figure 1, with those at LAR2 spanning ~2 years in 2007-9 and LAR1 and LAR3 spanning 2–3 months in 2007-8. We determined station positions every 300 s using the GIPSY v5.0 software [*Webb and Zumberge*, 1995] in precise point positioning mode and homogeneously reprocessed satellite orbits and clocks. We modeled solid earth tides and ocean tide loading displacements with accuracy ~1 mm. Coordinate time series for an onshore site at Palmer Station (~200 km away) suggest a precision of 5 mm (horizontal) and 10 mm (vertical) after removing signal with period <3 hours. For further analysis we rotated the north-east coordinate time series into along-across flow directions for each site.

[5] We show in Figure 2 (red lines) along-flow velocity, along-flow displacement (mean linear flow removed) and elevation for LAR2. The velocities have been computed from site displacements using a 2.5-day lowpass filter to remove the higher frequency signals, revealing fortnightly variation in velocity which is approximately ±10% of the mean annual velocity. The (unfiltered) along-flow displacement reveals signal at periods from a few hours to ~182 days, with the largest signals at 14.76 days and 182 days.

[6] In Figure 3 we show a 2-week portion of the series with the addition of LAR1 and LAR3 and now showing the more detailed high frequency velocities. Semidiurnal and diurnal velocity variations are ~±100% of the long-term velocity; that is the ice shelf occasionally flows upstream. The displacements (Figure 3b) show that the ice shelf at the three sites exhibits very similar flow variation amplitude across all periods, including 14.76 days. The mean velocities at LAR1 and LAR3 are higher than LAR2 but their fluctuations are remarkably similar. To investigate the phase and amplitudes of these signals more closely we performed a tidal decomposition [*Pawlowicz et al.*, 2002] of the complete time series of along-flow velocities. This is able to explain 93%, 89% and 95% of the variance of the along-flow velocities for LAR1-3, respectively, suggesting that the series are dominated by signals of tidal origin. In terms of velocity amplitude, the major tidal terms are given in Table 1. Due to record length, S_2 and MS_4 could only be determined reliably at LAR2. The vertical tide at M_{Sf} and MS_4 is <~0.01 m on LCIS, and since M_{Sf} and MS_4 may both be created through non-linear interaction of M_2 and S_2 [*Pugh*, 1987], the two largest vertical tidal constituents on the LCIS, this suggests that the tidal velocities have their origin in a non-linear process. Comparing amplitude spectra for the velocity (Figure S1a of the auxiliary material) and vertical motion (Figure S1b) highlights this nonlinear relationship.[1]

[7] We note that the sites have, within errors, identical M_{Sf} velocity amplitude and phase. A spatial pattern is evident in O_1 and M_2 whereby the signal at the two sites near the

[1]School of Civil Engineering and Geosciences, Newcastle University, Newcastle upon Tyne, UK.
[2]British Antarctic Survey, Cambridge, UK.

0094-8276/11/2011GL046680

[1]Auxiliary materials are available in the HTML. doi:10.1029/2011GL046680.

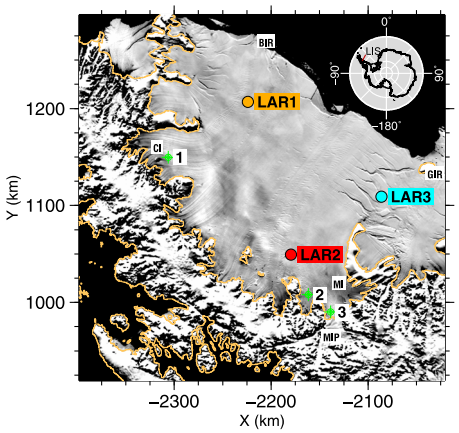

Figure 1. Larsen C Ice Shelf (Polar Stereographic projection) showing GPS sites (circles, colors matching the lines in Figure 3), tidal prediction locations (crosshairs) and background MOA [*Haran et al.*, 2005] image and grounding line (brown). Locations of Cabinet Inlet (CI), Mobiloil Inlet (MI), Mercator Ice Piedmont (MIP), Bawden Ice Rise (BIR) and Gipps Ice Rise (GIR) are also shown.

ice shelf front lags the signal at the site near the grounding line, but with larger amplitude. The amplitude difference is 50–75% for O_1 and ~30% for M_2. The difference in M_2 phase yields a speed of propagation from the grounding zone of ~100 m s^{-1}, much slower than a compressional wave in ice [*Blankenship et al.*, 1987] and hence some contribution is likely from one or more signals with spatial variation. The vertical tidal motion at all 3 sites is nearly identical, suggesting that any variation is not due to local tidal conditions.

[8] The variability in movement in the across-flow direction is much smaller than the along-flow variation. Indeed,

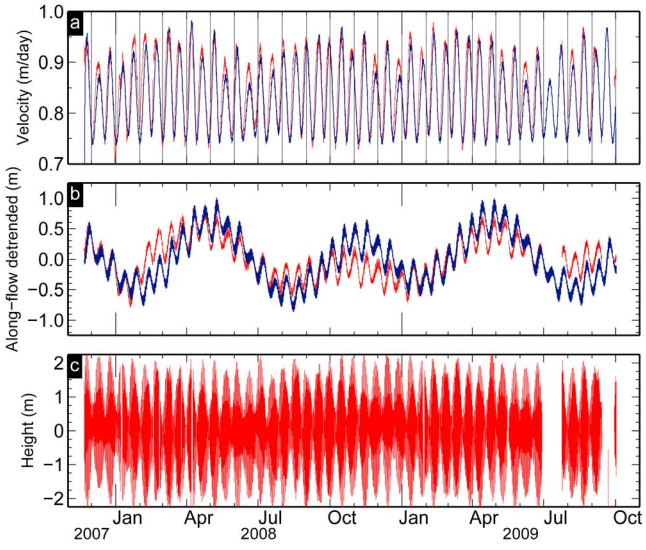

Figure 2. LAR2 site motion, showing (a) along-flow velocity low-pass filtered with a 2.5 day cutoff, (b) along-flow displacement (after removing mean linear flow), and (c) detrended height. Red lines are observed, blue (Figures 2a and 2b) are from the flow model.

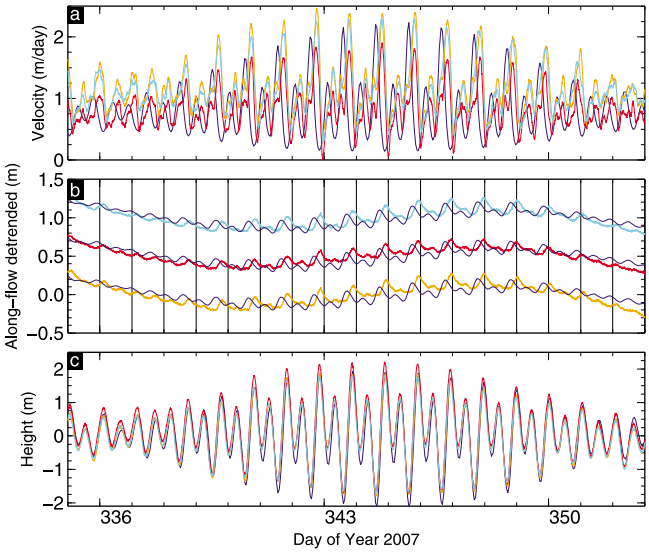

Figure 3. Site motion for LAR1 (orange), LAR2 (red) and LAR3 (cyan), showing (a) along-flow velocity low-pass filtered with a 3 hour cutoff, (b) along-flow displacement (after removing mean linear flow) with sites offset by 0.5 m for clarity, and (c) detrended height. Model estimates (blue) are also shown for LAR2 only (Figure 3a), all three sites (Figure 3b), and from CATS2008a (Figure 3c) evaluated for Cabinet Inlet (point 1 in Figure 1).

at LAR2 it is negligible whereas at LAR1 and LAR3 movement of a few centimeters is evident (Figure S2). Their structure, while being similar, is not identical to the along-flow motion, suggesting they have different origins.

[9] The signals at diurnal and semidiurnal periods suggest, therefore, that more than one tidal mechanism may be contributing to the observed modulation of ice flow at these periods. However, the long period signals point to a single non-linear mechanism relating to the tides, which is, within error, identical and synchronous across the entire ice shelf. The signature of observed along-flow velocity variations is remarkably similar to that seen on the floating Brunt Ice Shelf (update of *Doake et al.* [2002]) and the

Table 1. Results of Tidal Decomposition, Showing Only Terms With Observed Horizontal Amplitude ≥100 mm hr^{-1}, Plus MS_f[a]

			Amplitude (mm hr^{-1})		Phase (°)	
Constituent	Period	Site	Observed	Modeled	Observed	Modeled
MS_f	14.76 d	LAR1	97 ± 50		6 ± 33	
		LAR2	89 ± 3	86	14 ± 2	31
		LAR3	87 ± 9		14 ± 6	
O_1	25.82 hr	LAR1	181 ± 18		236 ± 5	
		LAR2	121 ± 3	161	229 ± 2	186
		LAR3	212 ± 18		230 ± 5	
M_2	12.42 hr	LAR1	350 ± 28		185 ± 5	
		LAR2	276 ± 11	522	167 ± 2	66
		LAR3	330 ± 23		176 ± 4	
K_1	23.93 hr	LAR2	140 ± 3	190	258 ± 1	193
S_2	12.00 hr	LAR2	209 ± 10	379	195 ± 3	97
MS_4	6.10 hr	LAR2	131 ± 7	83	70 ± 3	164

[a]Uncertainties are 95% confidence interval. Phase lags are positive. Model values for LAR1 and LAR3 are near identical to those for LAR2.

Table 2. Model Parameters[a]

Site	C (m d^{-1} kPa^{-m})	$\tilde{\tau}_b$ (kPa)	K	m	$\bar{u}_{tidal}$ (%)
LAR2	4.0×10^{-4}	10.0	−0.215	2.96	12.5%
Rutford ~40 km upstream [*King et al.*, 2010]	1.7×10^{-4}	17.6	±0.18	3	5.9%

[a] $\bar{u}_{tidal}$ is the component of mean velocity due solely to the presence of tides in the model.

grounded Rutford Ice Stream [*Gudmundsson*, 2006] each >1000 km distant. These both exhibit fortnightly variations in flow, with the Rutford also exhibiting variation from a few hours to ~182 days [*Gudmundsson*, 2007; *Murray et al.*, 2007] as seen here for LCIS. We note that the variations in flow rate are 50% larger than that observed on the Rutford [*Murray et al.*, 2007], although that site was ~40 km upstream. Tidal variations in flow have also been observed along the Siple Coast ice streams and on the Ross Ice Shelf [*Anandakrishnan et al.*, 2003; *Brunt et al.*, 2010], but they have different characteristics, possibly due to the different tidal regime there [*Gudmundsson*, 2010]. Since there is likely a single mechanism working at the longer periods, we continue by considering this aspect of the flow before returning to discuss the higher frequency signal.

3. Along-Flow Forcing Mechanism

[10] A number of potential mechanisms have so far been suggested that may be capable of producing tidal modulation of ice shelf flow. Unlike these, however, the dominant signal in our observations requires a nonlinear relation to tidal amplitude. The most likely geographical origin of this nonlinearity is in the ice shelf grounding zone along its western edge and this appears to be supported by the relative phases of the diurnal and higher frequency signal in our observations. However, the data are not entirely unambiguous in this matter and alternative source locations could include Bawden and Gipps ice rises near the ice shelf front (Figure 1).

[11] As an initial examination of the forcing mechanism we considered the possibility that the flow of the LCIS is forced, at least in part, by a non-linear response to tidal variations in the grounding zones of the glaciers flowing into the western edge of the ice shelf (Figure 1). We model the observed forward velocity (u_s) using a "Weertman" sliding law where velocity is proportional to some power of basal shear stress ($\tilde{\tau}_b$), but modified to allow a perturbation of $\tilde{\tau}_b$ that is linearly proportional to tidal height (h):

$$u_s = C(\tilde{\tau}_b + K\rho g h)^m \quad (1)$$

With C and K being constants of proportionality, m is the power law exponent, ρ = 1023 kg m^{-3} is the density of seawater and g = 9.81 m s^{-2} the acceleration due to gravity. This form of sliding law is suitable to both mountain glaciers [*Paterson*, 1994] and larger ice streams [*Gudmundsson*, 2007]. In equation (1) we follow *Gudmundsson* [2007] in assuming that tidal action affects basal stresses upstream of the grounding line, and that the corresponding perturbation is linearly related to tidal amplitude (h). The factor K in (equation (1)) is a site-dependent constant that accounts for the change in stress due to tidal action with distance away from the grounding line.

[12] We determined model parameters in equation (1) using data from LAR2, using the same approach as that of *King et al.* [2010]. (Records at the other sites are too short to derive stable model parameters). We fit the model to the filtered LAR2 2.5 d velocity series because we expected some signal in the semidiurnal and diurnal band which is not modeled by equation (1) [e.g., *Anandakrishnan et al.*, 2003]. This provides good constraint on all model parameters but leaves the solution insensitive to the sign of K which is most sensitive to high frequency terms [*King et al.*, 2010]. We expect the long period part of the LAR2 record to be representative of that experienced at its upstream grounding line (~50 km) as ice is viscous at these periods. To obtain a tidal height near to the grounding zone we used the CATS2008a model (updated from *Padman et al.* [2002]) evaluated at point 2 in Figure 1. We excluded long period tides (>~1 day) from the vertical tidal prediction.

[13] The determined model parameters are given in Table 2. We moderately constrained (±0.5) m to be 3.0, but it did not adjust away from this. We tried other values of m but these did not converge to a stable solution and so we consider the determined value to be robust.

[14] The modeled signal is shown in Figure 2 (blue line) after removing high frequency terms through low pass filtering. The mean velocity is reproduced closely by the model. The fortnightly variation in velocity signal (Figure 2a) closely matches the observed dominant fortnightly frequency and the phase is also very close with the model leading by ~17° (Table 1). These small errors integrate into the misfit observed in along-flow displacement (Figure 2b). Figure 3 allows a closer examination of the performance of the higher frequency components of the model. In terms of velocity (Figure 3a), comparing the red and blue lines suggests that the amplitudes of the highest frequency components are somewhat over-predicted in the model. The phase difference (Table 1) is ~50–100° for the dominant constituents, with the model leading by about 3–4 hours as a result.

[15] We also computed model estimates for LAR1 and LAR3 based on the LAR2 model parameters but forced by tides at the sites' respective upstream grounding zones (point 1 in Figure 1 for LAR1, point 3 for LAR3). Displacements (Figure 3b) were derived from the modeled velocity through integration and then detrended. The modeled response is nearly identical across all sites as the tidal forcing is also nearly identical (Figure 3c). The sub-daily structures of the modeled displacements are in close agreement with the observations, noting we did not fit the model to the observed signal in the sub-daily band as discussed above.

4. Discussion

[16] The model fit to the data is quite robust. The determined grounding zone basal stress is around 10 kPa which is significantly smaller than values typically quoted for alpine glaciers which range from ~60–80 kPa. The basal stress derived from the model (i.e., 10 kPa) is an estimate of the mean stress in the vicinity of the grounding line along the ice-till interface where the basal motion takes place. One can expect basal stress to be unevenly distributed over the glacier with higher stresses at the margins than at the

deepest part, and increasingly larger stresses upstream of the grounding line. In this context our estimate of around 10 kPa at the ice-till interface close to the grounding line does not seem unrealistic. Our derived value of $m \approx 3$ is in line with similar recent estimates for Rutford Ice Stream [*Gudmundsson*, 2007; *King et al.*, 2010] and hence is plausible; there is a paucity of estimates of m based on comparison between model and data, and our estimate adds to these.

[17] The model is capable of reproducing the observed tidally-induced variations in flow in some detail. The fit between model and data is particularly good over long tidal periods. Modeling the long-periodic variations is challenging because of the absence of any forcing at these frequencies. In the model the long-periodic variation in flow arises through a non-linear interaction between semi-diurnal and diurnal tidal components and the mechanism for this non-linearity is explained by the basal sliding law. Although we cannot exclude the possibility of other models being able to explain the observations, we are not aware of any with an established theory of nonlinear response to tidal forcing as is required by the data. However, given the importance of Gipps and Bawden ice rises to the long-term stability of the ice shelf system, further investigation is required into their role in modulating flow at the tidal frequencies we observe here.

[18] With this model, setting $h = 0$ in equation (1) gives the contribution of present-day mean velocity that comes from the presence of tides in the grounding zone. In this case, this equates to 12.5% of mean velocity, 2–3 times greater than that for Rutford Ice Stream (Table 2). If this were the only ice shelf force acting on the glacier, which it is not, then removing the glacier tidal forcing, for example due to breakup of the LCIS, would initially contribute to slowdown and thickening of inflowing glaciers.

[19] While fitting the long period signal well, the model does not, however, explain the entire signal. We suggest this is partly due to missing physics and partly due to at least one other mechanism which linearly depends on tides. The differences in phase between the model and the observations are most likely related to visco-elastic effects that are not described by the model. The model assumes a purely linear elastic response of the ice to loading over semi-diurnal and diurnal frequencies. *Reeh et al.* [2003] show that a more accurate description of ice rheology over tidal frequencies can be obtained using visco-elastic rheological models. Using such a model would give rise to a difference in predicted velocity phase and amplitude in the grounding zone compared to the model we employ [see *Gudmundsson*, 2010].

[20] In agreement with *Doake et al.* [2002], we dismiss a large role for ocean tide currents as the basal drag coefficient required to produce a sufficient amplitude would be unreasonably large and the frequency content provides a poor match to our observations. Furthermore, we dismiss a primary role of direct gravitational forcing as suggested by *Thomas* [2007] since, while the fortnightly tidal potential is largest at high latitudes, on LCIS it does not dominate the diurnal and semidiurnal potential as required to produce the observed signal (Figures 2 and 3).

[21] Grounding zone tidal model accuracy may also contribute to the misfit of the model. At present no tidal model attempts to model the grounding zone in which tides go from undamped, then damped and then to zero at the grounding line. The vertical tidal forcing at the grounding line is some function of the tidal forcing in the entire grounding zone, and it is this that should be used in equation (1). It is not clear if a simple linear relationship exists between the damped and the undamped tide, across all frequency bands. If it were a linear relationship it would be entirely absorbed by K. The misfit is notable at semi-annual periods (Figure 1), suggesting possible problems with one or more of S_2, K_2, K_1 or P_1 used to force the model [*King et al.*, 2010]. Tidal models which accurately capture the grounding zone are therefore required.

[22] The across-flow variations suggest an influence of tidal tilting of the ice shelf (Figure S2), a mechanism proposed by *Thomas* [2007]. The qualitative agreement between the across-flow tilt (grey lines) and the across-flow movement at both LAR1 and LAR3 is high. The magnitude of the LAR3-LAR1 tilt shown is equivalent to ±0.07°. The phase difference between the tilt and LAR1 motion is ~10 minutes. LAR3 lags LAR1 in its motion by about 40 minutes, although the phase lag is less as the ice shelf tilts toward LAR1 and greater as it tilts toward LAR3. The large rifts near LAR3 (Figure 1) may be important, as may be the proximity of LAR2 to the grounding zone in mitigating the effect. Clearly this requires modeling, but if similar tidal tilt effects were to be shown in the along-flow direction (dark line, Figure S2) we suggest it may help explain the amplification of the diurnal and semidiurnal signals at LAR1 and LAR3 compared to LAR2.

5. Conclusions

[23] We observe periodic variation in the speed of Larsen C Ice Shelf of up to 100% of its long-term mean. Comparison of the amplitudes of the velocity variation with vertical tidal forcing reveals a nonlinear relationship. The non-linear aspect of the observations can be explained by assuming that the vertical tidal motion of the ice shelf affects the basal stress regime of the tributaries some distance upstream from the grounding line, and, furthermore, that the relationship between basal stress and basal motion follows a non-linear sliding law. We find that using a Weertman type sliding law with moderately large stress exponent gives modeled displacement curves that closely follow the observed ones. The model fits the observed 14.76 d and 182 d amplitude and phase, as well as the higher frequency signal structure, but cannot replicate the phase of the semi-diurnal and diurnal signal or its amplification toward the ice shelf front. We suggest viscoelastic effects may contribute to the former and tidal tilt of the ice shelf to the latter. Although both of these effects (viscoelasticity and tidal tilt) are not accounted for in the model, including them is not expected to affect the modeled response at the long-tidal periods. Our model presupposes the presence of long-periodic modulation on the Larsen C tributaries. Collecting further GPS data from the tributaries will allow this assumption to be tested.

[24] **Acknowledgments.** This work was funded by NERC AFI and GEF grants/loans and a RCUK Academic Fellowship to MAK. We thank David Barber and BAS logistics, pilots and field assistants for deploying (and digging out) the equipment. The manuscript was significantly

improved through comments by Doug MacAyeal, Robert H. Thomas, anonymous reviewers and Eric Rignot (Editor).

[25] The Editor thanks three anonymous reviewers for their assistance in evaluating this paper.

References

Anandakrishnan, S., D. E. Voigt, R. B. Alley, and M. A. King (2003), Ice stream D flow speed is strongly modulated by the tide beneath the Ross Ice Shelf, *Geophys. Res. Lett.*, *30*(7), 1361, doi:10.1029/2002GL016329.

Blankenship, D. D., C. R. Bentley, S. T. Rooney, and R. B. Alley (1987), Till beneath Ice Stream B: 1. Properties derived from seismic travel times, *J. Geophys. Res.*, *92*(B9), 8903–8911, doi:10.1029/JB092iB09p08903.

Brunt, K. M., M. A. King, H. A. Fricker, and D. R. MacAyeal (2010), Flow of the Ross Ice Shelf, Antarctica, is modulated by the ocean tide, *J. Glaciol.*, *56*(195), 157–161, doi:10.3189/002214310791190875.

Doake, C. S. M., H. F. J. Corr, K. W. Nicholls, A. Gaffikin, A. Jenkins, W. I. Bertiger, and M. A. King (2002), Tide-induced lateral movement of Brunt Ice Shelf, Antarctica, *Geophys. Res. Lett.*, *29*(8), 1226, doi:10.1029/2001GL014606.

Glasser, N. F., B. Kulessa, A. Luckman, D. Jansen, E. C. King, P. R. Sammonds, T. A. Scambos, and K. C. Jezek (2009), Surface structure and stability of the Larsen C ice shelf, Antarctic Peninsula, *J. Glaciol.*, *55*(191), 400–410, doi:10.3189/002214309788816597.

Gudmundsson, G. H. (2006), Fortnightly variations in the flow velocity of Rutford Ice Stream, West Antarctica, *Nature*, *444*(7122), 1063–1064, doi:10.1038/nature05430.

Gudmundsson, G. H. (2007), Tides and the flow of Rutford Ice Stream, West Antarctica, *J. Geophys. Res.*, *112*, F04007, doi:10.1029/2006JF000731.

Gudmundsson, G. H. (2010), Ice-stream response to ocean tides and the form of the basal sliding law, *Cryosphere Discuss.*, *4*(4), 2523–2555, doi:10.5194/tcd-4-2523-2010.

Haran, T., J. Bohlander, T. Scambos, and M. Fahnestock (2005), MODIS mosaic of Antarctica (MOA) image map, edited, Natl. Snow and Ice Data Cent., Boulder, Colo.

King, M. A., T. Murray, and A. M. Smith (2010), Non-linear responses of Rutford Ice Stream to semi-diurnal and diurnal tidal forcing, *J. Glaciol.*, *56*(195), 167–176, doi:10.3189/002214310791190848.

Murray, T., A. M. Smith, M. A. King, and G. P. Weedon (2007), Ice flow modulated by tides at up to annual periods at Rutford Ice Stream, West Antarctica, *Geophys. Res. Lett.*, *34*, L18503, doi:10.1029/2007GL031207.

Padman, L., H. A. Fricker, R. Coleman, S. Howard, and L. Erofeeva (2002), A new tide model for the Antarctic ice shelves and seas, *Ann. Glaciol.*, *34*(1), 247–254, doi:10.3189/172756402781817752.

Paterson, W. S. B. (1994), *The Physics of Glaciers*, 3rd ed., 480 pp., Elsevier Sci., Oxford, U. K.

Pawlowicz, R., B. Beardsley, and S. Lentz (2002), Classical tidal harmonic analysis including error estimates in MATLAB using T_TIDE, *Comput. Geosci.*, *28*(8), 929–937, doi:10.1016/S0098-3004(02)00013-4.

Pugh, D. T. (1987), *Tides, Surges and Mean Sea-Level: A Handbook for Engineers and Scientists*, 472 pp., John Wiley, Chichester, U. K.

Reeh, N., E. L. Christensen, C. Mayer, and O. B. Olesen (2003), Tidal bending of glaciers: a linear viscoelastic approach, *Ann. Glaciol.*, *37*(1), 83–89, doi:10.3189/172756403781815663.

Rignot, E., G. Casassa, P. Gogineni, W. Krabill, A. Rivera, and R. Thomas (2004), Accelerated ice discharge from the Antarctic Peninsula following the collapse of Larsen B ice shelf, *Geophys. Res. Lett.*, *31*, L18401, doi:10.1029/2004GL020697.

Scambos, T., C. Hulbe, and M. Fahnestock (2004), Climate-induced ice shelf disintegration in the Antarctic Peninsula, in *Antarctic Peninsula Climate Variability: Historical and Paleoenvironmental Perspectives*, *Antarct. Res. Ser.*, vol. 79, edited by E. Domack et al., pp. 79–92, AGU, Washington, D. C.

Thomas, R. H. (2007), Tide-induced perturbations of glacier velocities, *Global Planet. Change*, *59*(1–4), 217–224, doi:10.1016/j.gloplacha.2006.11.017.

Webb, F. H., and J. F. Zumberge (1995), An introduction to GIPSY/OASIS-II precision software for the analysis of data from the Global Positioning System, *JPL Publ.*, *D-11088*.

G. H. Gudmundsson and K. Makinson, British Antarctic Survey, High Cross, Madingley Road, Cambridge CB3 0ET, UK.

M. A. King, School of Civil Engineering and Geosciences, Newcastle University, Cassie Building, Newcastle upon Tyne NE1 7RU, UK. (m.a.king@newcastle.ac.uk)